Human Molecular Genetics, 2008, Vol. 17, No. 24 ***3909–3918***
doi:10.1093/hmg/ddn293
Advance Access published on September 10, 2008

Cell-penetrating peptide-conjugated antisense oligonucleotides restore systemic muscle and cardiac dystrophin expression and function

HaiFang Yin[1], Hong M. Moulton[2], Yiqi Seow[1], Corinne Boyd[1], Jordan Boutilier[2], Patrick Iverson[2] and Matthew J.A. Wood[1,*]

[1]Department of Physiology, Anatomy and Genetics, University of Oxford, South Parks Road, Oxford OX1 3QX, UK and [2]AVI Biopharma Inc., Corvallis, OR, USA

Received June 30, 2008; Revised and Accepted September 9, 2008

Antisense oligonucleotides (AOs) have the potential to induce functional dystrophin protein expression via exon skipping by restoring in-frame transcripts in the majority of patients suffering from Duchenne muscular dystrophy (DMD). AOs of morpholino phosphoroamidate (PMO) and 2′-*O*-methyl phosphorothioate RNA (2′*O*me RNA) chemistry have been shown to restore dystrophin expression in skeletal muscle but not in heart, following high-dose systemic delivery in murine models of muscular dystrophy (*mdx*). Exploiting the cell transduction properties of two basic arginine-rich cell penetrating peptides, we demonstrate widespread systemic correction of dystrophin expression in body-wide muscles and cardiac tissue in adult dystrophic *mdx* mice, with a single low-dose injection of peptide-conjugated PMO AO. This approach was sufficient to restore uniform, high-level dystrophin protein expression in peripheral muscle and cardiac tissue, with robust sarcolemmal relocalization of the dystrophin-associated protein complex and functional improvement in muscle. Peptide-conjugated AOs therefore have significant potential for systemic correction of the DMD phenotype.

INTRODUCTION

Duchenne muscular dystrophy (DMD) is a severe muscle degenerative disorder characterized by mutations that disrupt the reading frame in the dystrophin (*DMD*) gene leading to the absence of functional protein (1). A related allelic disorder, Becker muscular dystrophy (BMD), is caused by mutations that give rise to shortened but in-frame transcripts resulting in the production of truncated but partially functional protein. Such partially functional protein retains the critical amino terminal, cysteine rich and C-terminal domains but usually lacks elements of the central rod domains which are of less functional significance (2). As a consequence, BMD phenotypes range from mild DMD to virtually asymptomatic, depending on the precise mutation and the level of dystrophin produced.

Antisense oligonucleotide (AO)-mediated splice modification of out-of-frame dystrophin transcripts has been demonstrated to exclude specific dystrophin exons, thereby restoring the open reading frame and resulting in the production of Becker-like, shortened but partially functional dystrophin protein (3–13). Utilizing 2′*O*-methyl modified oligonucleotides delivered by direct intramuscular injection, Lu *et al.* (8) demonstrated molecular correction of a dystrophin transcript in *mdx* mice bearing a nonsense mutation in exon 23, resulting in local dystrophin production and functional improvement. Proof-of-principle for this therapeutic approach has also been successfully shown in human subjects using a similar local intramuscular AO-injection protocol (11).

To develop AO-mediated exon-skipping as an effective therapy for DMD will require systemic correction of the molecular defect, including in cardiac muscle. Given that cardiomyopathy is a significant cause of morbidity and death in DMD patients, restoration of dystrophin expression in heart is a critical requirement for successful exon skipping therapy (14,15). Previous work has shown that alternative chemistry phosphorodiamidate morpholino oligomers (PMO) are capable of restoring dystrophin expression in multiple muscle groups following systemic intravenous delivery in *mdx* mice, but this

*To whom correspondence should be addressed. Tel: +44 1865272419; Fax: +44 1865272420; Email: matthew.wood@dpag.ox.ac.uk

required a high-dose multi-injection protocol and molecular correction in cardiac muscle was not observed (4).

Short, positively charged arginine-rich peptides have been shown to function as cell penetrating peptides, enhancing the cell uptake of a variety of cargoes including oligonucleotides (16). Such peptide–oligonucleotide conjugates have been previously demonstrated to effect splice correction of mutant dystrophin transcripts in cell culture and also in neonatal *mdx* mice via intraperitoneal injection, demonstrating their potential for enhancing the delivery and exon-skipping efficacy of AOs (17,18). Here we evaluate two arginine-rich peptide-PMO conjugates in adult *mdx* mice by systemic intravenous injection and demonstrate highly effective and widespread dystrophin correction in multiple peripheral skeletal muscles and in cardiac muscle, at low systemic AO doses.

RESULTS

To test whether improved systemic AO delivery and cardiac dystrophin correction could be obtained in *mdx* dystrophic mice, we investigated a previously described arginine-rich peptide-PMO conjugate, P007-PMO, and a novel conjugate B-PMO (see Table 1 for AO and peptide sequence information). Peptides were conjugated to PMO AOs targeting the murine dystrophin exon 23 5′ splice donor site, using an established 25mer target sequence. Conjugates were evaluated initially by intramuscular delivery into adult 6–8-week-old *mdx* tibialis anterior (TA) muscles and demonstrated to promote high levels of dystrophin protein restoration as shown by the widespread dystrophin-positive muscle fibres throughout muscle cross-sections by immunostaining (Supplementary Material, Fig. S1) and western blot (data not shown). We then went on to evaluate these compounds by systemic intravenous delivery in adult *mdx* mice.

Single low-dose PMO-peptide conjugates restore dystrophin expression in muscle and cardiac tissue

Given the high-level intramuscular correction obtained with the two PMO-peptide conjugates, we therefore investigated whether single intravenous injections of these PMO conjugates could restore dystrophin expression systemically. A 25 mg/kg single injection administration protocol was tested with the P007-PMO conjugate administered via the mouse tail vein. Three weeks following single injections, all skeletal muscle fibres immunostained positive for sarcolemmal dystrophin. The intensity of dystrophin expression was near normal in most skeletal muscle groups analysed, although slightly lower in biceps as shown (Fig. 1A). Widespread, uniform expression of dystrophin protein over multiple tissue sections within each muscle group was detected in hind limb, fore limb, abdominal wall and diaphragm muscles. Surprisingly, no obvious area-to-area variation was found within individual muscle groups as previously reported with the systemic delivery of naked PMO AOs (4). RT-PCR results revealed almost total exon skipping of the mutated transcript with highly effective skipping of *mdx* dystrophin exon 23 (Fig. 1B) in all skeletal muscles analysed including the diaphragm. Less efficient molecular correction was observed in heart, where ~50% of the mutated transcript was found to be exon skipped by RT-PCR. A shorter band was also detected in the RT-PCR assay in many analysed tissues, which was likely to correspond to a skipped transcript lacking exons 22 and 23. Subsequent sequencing of this PCR fragment confirmed that the minor transcript product contained exon 22 and 23 deletions (data not shown). To quantify the levels of dystrophin protein restored, western blot analysis was undertaken, using total protein extracted from all muscle groups including heart, and from normal C57 TA and heart muscle tissues as positive controls. This indicated that between 25 and 100% of normal dystrophin protein levels had been restored in body-wide skeletal muscles following the single systemic AO injection. Of particular significance were the levels approaching 100% restoration of dystrophin protein that were detected in distal muscle groups, i.e. TA and biceps, while even in the diaphragm almost 25% of normal dystrophin protein was restored (Fig. 1C).

Cardiac tissue from treated mice was also analysed by immunostaining and this too demonstrated widely distributed dystrophin-positive fibres throughout the cardiac muscle (Fig. 1A). Dystrophin protein restoration was not found to be as high in heart as for peripheral skeletal muscle groups but levels of between 10 and 20% of that found in normal mouse heart were typically seen by western analysis in all treated animals (Fig. 1D). This is the first demonstration of widespread dystrophin protein correction in the *mdx* mouse heart with such low AO doses.

Comparison of P007-PMO with other arginine-rich PMO peptide conjugates

P007-PMO contains alternating arginine and non-natural 6 aminohexanoic acid amino acids in an $(RXR)_4$ sequence. To test the efficacy of further modified arginine-rich PMO-peptide conjugates, we directly compared a second conjugate (B-PMO) containing a transduction peptide in which two 6 aminohexanoic acid residues were substituted with β-alanine residues, a second non-natural amino acid (see peptide sequences in Table 1). Taking the same approach, B-PMO delivered by intravenous delivery also demonstrated highly effective systemic dystrophin correction in skeletal muscle and cardiac tissue but with a lower efficiency than the P007-PMO AO at the same dose, as shown by western analysis (Supplementary Material, Fig. S2).

Evaluation of a lower-dose intravenous P007-PMO dosing protocol to optimize dystrophin correction

Our RT-PCR data above showed almost complete exon skipping at the RNA level in the majority of skeletal muscles following treatment with a 25 mg/kg AO dose, suggesting the possibility that the AO dose had reached near saturation in these tissues. Given this finding and that the half-life of dystrophin protein *in vivo* has been estimated at up to 26 weeks in *mdx* mice (19), we decided to test whether modifications to the AO delivery protocol to include multiple lower-dose injections could improve molecular dystrophin correction without AO dose saturation in skeletal muscles. A protocol of weekly injections of P007-PMO at 6 mg/kg for 3 weeks resulted in a lower total AO dose administered and significantly improved

Table 1. Oligonucleotide and peptide nomenclature and sequences

Name	Sequence	Abbreviation	Length
M23D	5′-GGCCAAACCTCGGCTTACCTGAAAT-3′	PMO	25
P007	N- RXRRXRRXRRXRXB -C	$(RXR)_4XB$	14
B peptide	N- RXRRBRRXRRBRXB -C	$(RXRRBR)_2XB$	14

R, L-arginine; X, 6-aminohexanoic acid; B, β-alanine.

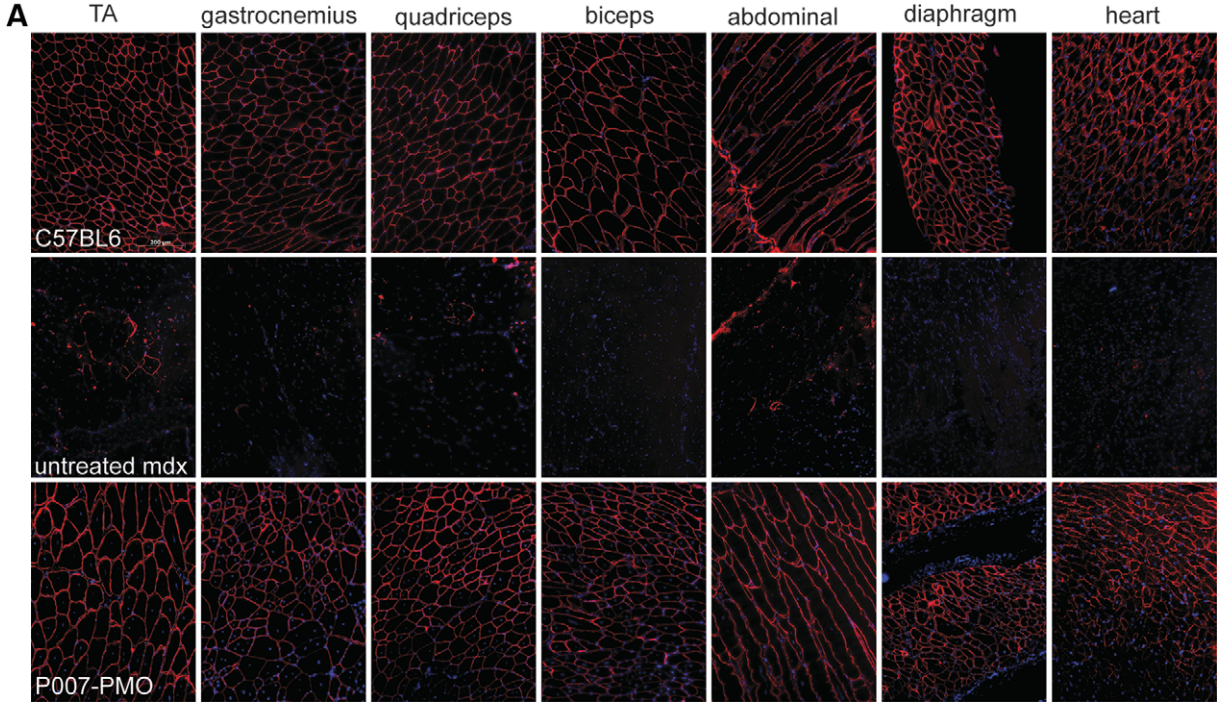

Figure 1. Restoration of muscle and cardiac dystrophin expression in *mdx* mice. Restoration of dystrophin expression following single 25 mg/kg intravenous injections of the P007-PMO AO conjugate in adult *mdx* mice. (**A**) Immunostaining of muscle tissue cross-sections to detect dystrophin protein expression and localization in C57BL6 normal control mice (top panel), untreated *mdx* mice (middle panel) and P007-PMO-treated *mdx* mice (lower panel), showing near normal levels of dystrophin expression in the treated mice. Muscle tissues analysed were from tibialis anterior (TA), gastrocnemius, quadriceps, biceps, abdominal wall, diaphragm and heart muscles (scale bar = 200 μm). (**B**) RT-PCR to detect exon skipping efficiency at the RNA level demonstrated almost complete exon 23 skipping in the peripheral skeletal muscles indicated and ∼50% exon skipping in heart in treated *mdx* mice. This is shown by shorter exon-skipped bands (indicated by the boxed numbered 22–24—for exon 23 skipping). Truncated transcripts deleted for both exons 22 and 23 were also seen as indicated by the box 21–24. (**C**) Western blot for dystrophin expression in peripheral skeletal muscles showed ∼100% dystrophin restoration in all skeletal muscles except the diaphragm and with P007-PMO conjugate treatment compared with levels found in normal C57BL6 mice. Equal loading of 10 μg protein is shown for each sample with α-actinin expression detected as a loading control. (**D**) Western blot to detect dystrophin expression in heart tissue from normal C57BL6 heart (20, 10 and 5% of normal levels shown), untreated *mdx* heart and P007-PMO treated heart. Data shows dystrophin protein restoration to ∼15% of normal levels in treated *mdx* heart tissue.

molecular correction compared with age-matched controls in body-wide muscles as shown by immunostaining (Fig. 2A). High levels of dystrophin expression were detected in TA, quadriceps and gastrocnemius muscles, comparable with that found following the 25 mg/kg dose. The most striking differences were seen in the abdominal wall muscles, diaphragm and heart, where a lower level of dystrophin correction was found with the 6 mg/kg dose regime compared with the 25 mg/kg dose. RT-PCR results were consistent with the immunostaining data, again showing almost complete exon 23 skipping in TA, quadriceps and gastrocnemius muscles, but only ∼50% exon skipping efficiency in diaphragm and abdominal wall muscles, with even less dystrophin exon 23 skipping detectable in heart, although dystrophin-positive fibres were observed in the cardiac tissue by immunostaining (Fig. 2B). The western blot data demonstrated a lower level of protein restoration in abdominal wall, diaphragm and heart tissues, compared with that seen following the 25 mg/kg treatment, consistent with the RT-PCR and immunostaining findings (Fig. 2C). In this lower-dose study, we also compared the second peptide-PMO conjugate—B-PMO—using the same approach, with the results again confirming that the P007-PMO compound had superior activity to B-PMO as determined at both RNA (data not shown) and protein levels (Supplementary Material, Fig. S2C).

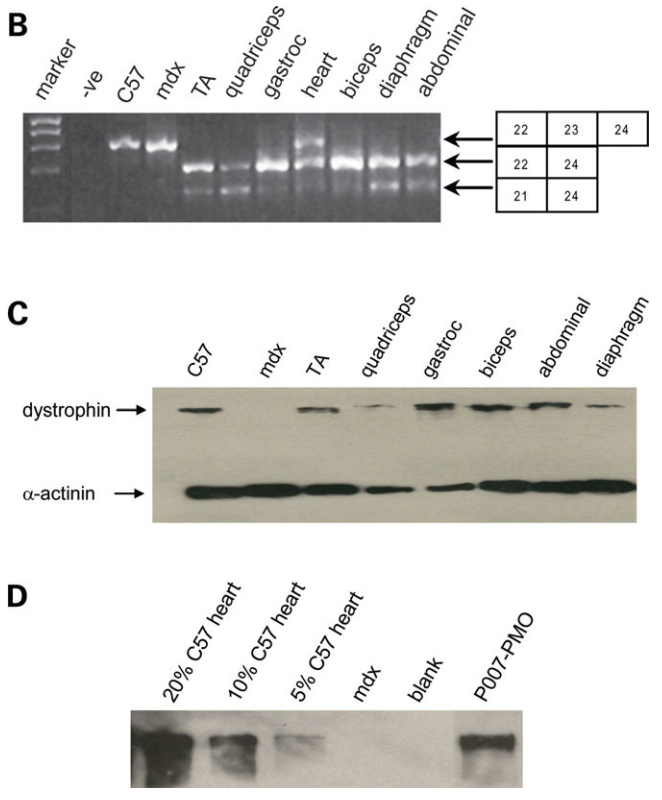

Figure 1. Continued

Functional correction in skeletal muscle following systemic delivery of the P007-PMO conjugate

Dystrophin plays a critical role in muscle by linking cytoplasmic actin to a sarcolemmal dystrophin-associated protein complex (DAPC) and via this to the extracellular matrix (20,21). The DAPC also has important signalling functions via nNOS and other components (22,23). In the absence of functional dystrophin the DAPC fails to localize accurately to the sarcolemma and its function is compromised. We therefore investigated whether restored dystrophin protein expression via systemic P007-PMO delivery resulted in the successful relocalization of DAPC protein constituents to the sarcolemma. As expected, the expression of multiple DAPC component proteins including β-dystroglycan, α-sarcoglycan and β-sarcoglycan and nNOS, was detected in peripheral skeletal muscles with correct sarcolemmal localization and with staining intensities commensurate with that observed for dystrophin at the 25 mg/kg dose (Fig. 3A). The restoration of DAPC components was also observed in the 6 mg/kg dose study although at a correspondingly lower level of expression (data not shown).

As a result of successfully restored dystrophin and DAPC expression we then wished to determine whether any evidence of improved muscle function could be detected. Using a functional test of grip force strength (24–26), evaluating predominantly but not exclusively forelimb muscle strength, *mdx* mice treated with P007-PMO AO were shown to have significantly improved grip strength to within the normal range following a 25 mg/kg dose, compared with untreated *mdx* control mice (Fig. 3B). Some improvement was also detected in *mdx* mice treated with the 6 mg/kg P007-PMO dose but it was not as great as that seen following the 25 mg/kg treatment (data not shown). The percentage of muscle fibres with centrally located nuclei is an index of ongoing degeneration/regeneration cycles (27,28). Counts of centrally located nuclei within treated *mdx* muscle groups (TA, gastrocnemius and quadriceps) revealed a significant reduction in centrally nucleated myofibres compared with untreated control *mdx* mice, suggesting a reduced regenerative stimulus and restoration of normal myofibre architecture commensurate with improved function (Fig. 3C). There was also a significant fall in the number of centrally nucleated fibres in TA and gastrocnemius muscles at the 6 mg/kg dose (data not shown). Serum creatine kinase (CK) levels are elevated in *mdx* mice and are indicative of ongoing muscle pathology and membrane instability (29). The significantly lower levels of serum CK found in P007-PMO treated *mdx* mice compared with untreated controls indicated the widespread protection effect of restored dystrophin expression on myofibre integrity (Fig. 3D).

Investigation of toxicity following treatment with the P007-PMO conjugates

Mdx mice treated with the peptide-PMO conjugates demonstrated no obvious outward signs of ill health. In order to further monitor any potential systemic cytotoxicity induced by the PMO and/or conjugated peptides, we undertook histological study of liver and kidney tissues and analysed a series of serum markers commonly used as indices of liver and kidney dysfunction. Haematoxylin and eosin staining of liver and kidney tissue sections did not reveal overt signs of tissue damage in *mdx* mice treated with P007-PMO conjugate, with no deleterious changes detectable in tissue morphology or increase in the numbers of infiltrating cells compared with untreated *mdx* control mice. Of particular interest was the liver histology where not only was no evidence of toxicity found following treatment, but a reversal of the typical swollen hepatic cell pathology (30) found in untreated *mdx* mice was seen (Fig. 4A). Serum was collected from treated *mdx* mice and control mice, and this showed a significant decrease in the levels of aspartate aminotransferase (AST) and alanine aminotransferase (ALT) liver enzymes in the treated mice, with levels of these enzymes returned to within the normal range compared with untreated *mdx* mice and normal age-matched untreated control mice (Fig. 4B). No change was found in the serum levels of urea and creatinine with P007-PMO treatment compared with untreated *mdx* controls and normal mice (data not shown) suggesting no adverse effects of the P007-PMO treatment on renal function at the doses studied. Overall these results indicated that over the course of the experiment, the P007-PMO conjugate did not induce any overt hepatic or renal toxicity at the systemic dose of 25 mg/kg in *mdx* mice. No signs of toxicity were observed with 6 mg/kg dose regime (data not shown).

DISCUSSION

In this report we demonstrate effective systemic dystrophin correction in adult *mdx* dystrophic mice in both peripheral

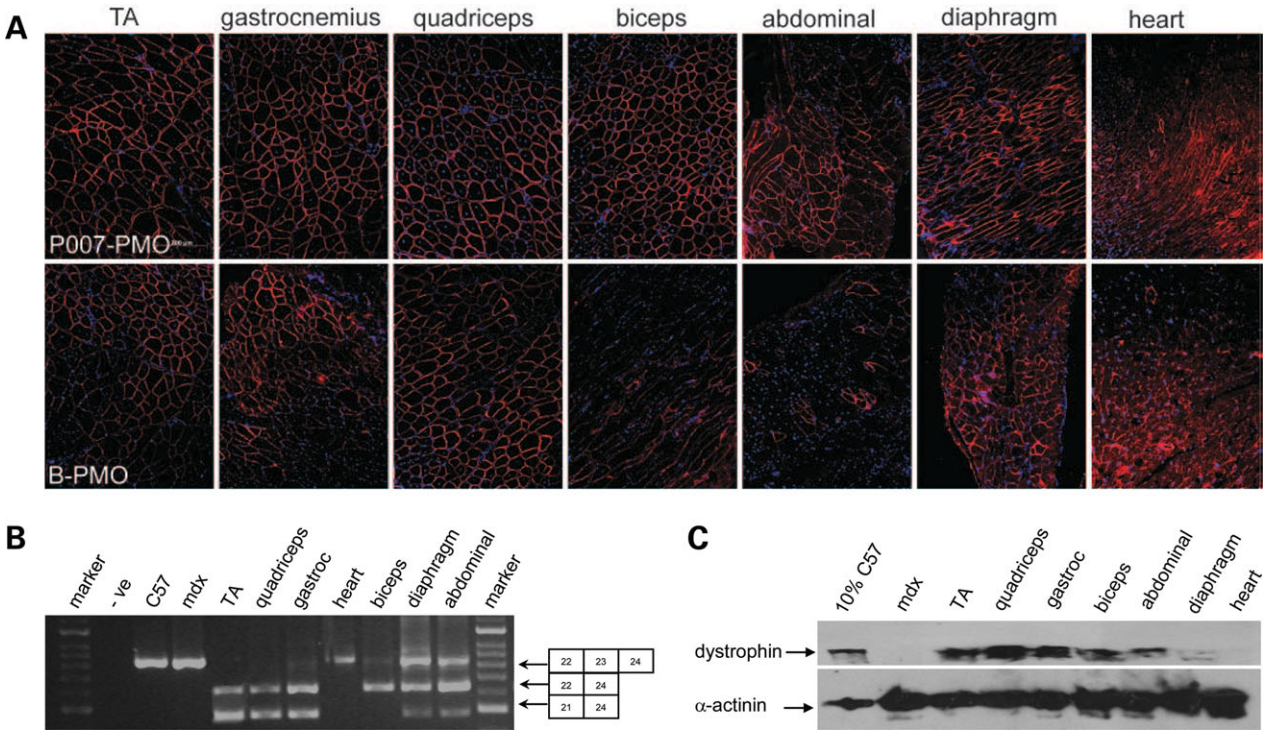

Figure 2. Body-wide dystrophin restoration in skeletal muscles of adult *mdx* mice with a PMO-peptide dose of 6 mg/kg. (**A**) Immunohistochemistry to detect dystrophin expression and localization in peripheral muscles from *mdx* mice treated with either P007-PMO (upper panel) or B-PMO (lower panel) at the 6 mg/kg dose. Data for control normal C57BL6 and untreated *mdx* mice are shown in Figure 1A. Muscle tissues analysed were from tibialis anterior (TA), gastrocnemius, quadriceps, biceps, abdominal wall, diaphragm and heart muscles (scale bar = 200 μm). High numbers of dystrophin-positive fibres are detected in cross-sections within the skeletal muscles but not in heart. (**B**) RT-PCR to detect the dystrophin exon skipping products in various treated *mdx* muscle groups as shown; unskipped or deleted for exon 23 or exon 22 and 23 as indicated in the boxes. Results show almost no full-length dystrophin transcript is detectable in TA, quadriceps and gastrocnemius (indicated by boxed number 22–24), with ∼50% exon 23 skipping in abdominal muscle and diaphragm and less in heart. (**C**) Western blot to detect dystrophin protein in the indicated muscle groups from treated *mdx* mice compared with C57BL6 and untreated *mdx* control mice. Data shows up to 30% dystrophin expression in quadriceps and gastrocnemius, but lower levels in diaphragm and less in heart. Equal loading of 50 μg protein is shown for each sample except for C57BL6 control lane where 5 μg of protein was loaded. α-actinin expression was detected as a loading control.

skeletal muscle and cardiac tissue using PMO AOs conjugated to arginine-rich peptides, administered at low systemic doses. A single 25 mg/kg intravenous dose of PMO-peptide conjugate was sufficient to rescue high levels of sarcolemmal dystrophin protein, DAPC component re-localization and histological and functional correction, with the P007-PMO conjugate demonstrating the greater efficacy. This highlights the potential of PMO-peptide conjugates as compounds with therapeutic value for body-wide and cardiac dystrophin correction and is corroborated in a recent report of a related conjugate (31). Clinical studies to evaluate AO exon skipping in DMD patients are in progress in both The Netherlands (11) and the UK, using 2′*O*-methyl phosphorothioate and PMO AO compounds, respectively. AO-peptide conjugates therefore offer the possibility of efficient systemic and cardiac dystrophin correction at significantly lower doses than previously used for unconjugated AOs in *mdx* mice (4), reducing possible concerns regarding potential toxicity of high dose 2′*O*-methyl phosphorothioate and PMO AOs in human subjects and the cost of AOs. While further studies are warranted to fully investigate the toxicological profile of the transduction peptides used in this report, we found no evidence of systemic toxicity in treated *mdx* mice over the course of the experiments.

Previous work investigating PMO-based exon skipping in adult *mdx* mice failed to find evidence of cardiac dystrophin correction even at a very high multiple doses of 100 mg/kg (4,18). Our data demonstrating widespread dystrophin correction in heart, with protein levels restored up to 20% of normal at 3 weeks following single intravenous AO injections, shows that there is no intrinsic barrier to cardiac dystrophin correction in *mdx* mice using AO therapeutic agents (indeed high efficiency AO-mediated exon skipping can be achieved in primary *mdx* cardiomyocytes; Walker, Wood and Yin, unpublished data). Given that correction of the cardiac defect due to loss of dystrophin protein is an essential component of a successful DMD therapy (14,15) and that therapies restoring dystrophin in skeletal muscles but not in cardiac muscle may exacerbate the underlying cardiac pathology (32), PMO-peptide conjugates have significant potential for systemic correction of the DMD phenotype. The mechanism by which the arginine-rich $(RXR)_4$ transduction peptide facilitates cardiac AO delivery and efficacy within that tissue remains unclear. Such cationic peptides are thought to bind to cell-associated glycosaminoglycans to be subsequently internalized by endocytosis (16), thus the mechanism by which such biochemical events may lead to enhanced transvascular AO delivery to

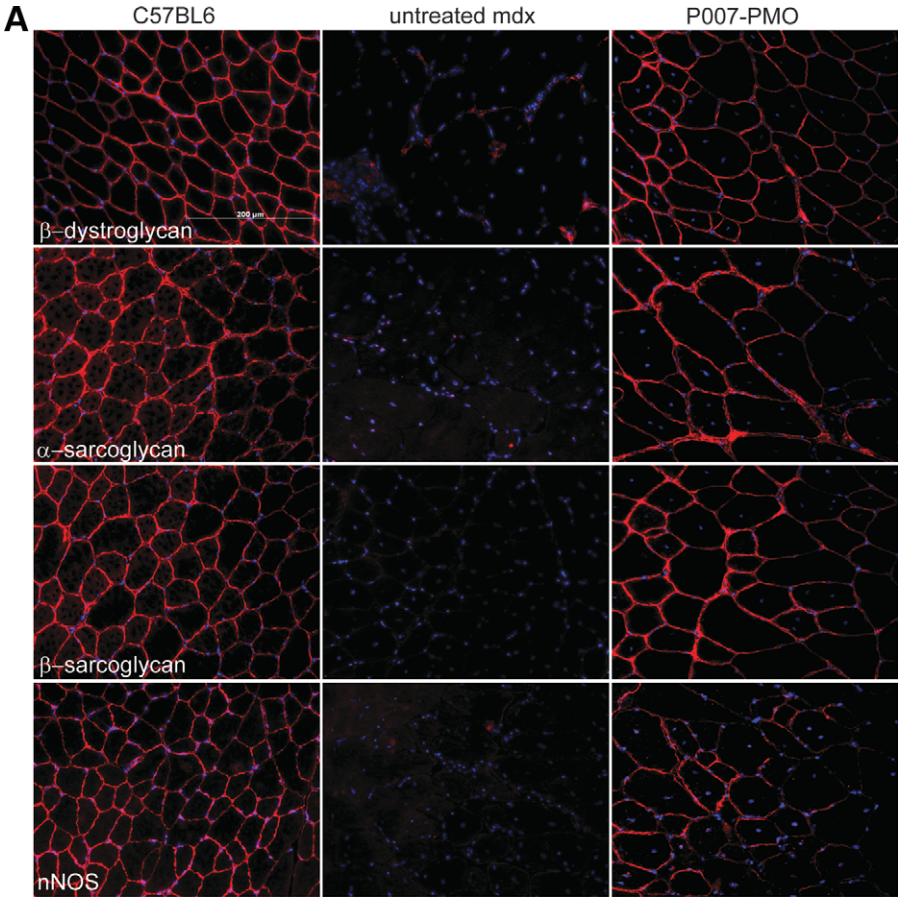

Figure 3. Functional evaluation of *mdx* skeletal muscles following treatment with the P007-PMO conjugate. (**A**) Restoration of the dystrophin-associated protein complex (DAPC) in *mdx* mice treated with P007-PMO at 25 mg/kg was studied to assess dystrophin function and recovery of normal myoarchitecture. DAPC protein components β-dystroglycan, α and β-sarcoglycan and nNOS were detected by immunostaining in tissue cross-sections of TA muscles from treated *mdx* mice compared with C57BL6 normal mice and untreated *mdx* control mice. All detected DAPC components are found to be successfully re-localized to the *mdx* muscle sarcolemma after treatment. (**B**) Muscle function was assessed using a functional grip strength test to determine the physical improvement of P007-PMO treated *mdx* mice compared with C57BL6 and untreated *mdx* mice. Data shows significant functional improvement in treated *mdx* mice with functional recovery observed into the normal range seen in untreated age-matched control mice ($P < 0.005$). (**C**) Evaluation of the numbers of centrally nucleated myofibres in TA, gastrocnemius and quadriceps muscles following a P007-PMO treatment compared with the corresponding untreated *mdx* muscles. Data shows a significant decrease in the number of centrally nucleated myofibres in treated *mdx* muscles compared with controls ($P < 0.005$). (**D**) Measurement of serum creatine kinase (CK) levels as an index of ongoing muscle membrane instability in treated *mdx* mice compared with normal and *mdx* control mice. Data show a significant fall in the serum CK levels in *mdx* mice treated with P007-PMO compared with untreated age-matched *mdx* controls ($n = 6$ for treated group and $n = 4$ for control, $P < 0.05$).

cardiac and muscle tissue is not understood. Nevertheless, highly efficient cardiac and muscle gene delivery can be achieved using AAV vectors (33,34), including the delivery of splice correcting DNA constructs (35), and therefore it seems plausible that arginine-rich transduction peptides permit efficient transvascular AO tissue entry to these tissues via similar mechanisms. While re-administration of peptide-PMO AOs will be required, our data suggests that similar levels of cardiac dystrophin correction may be achievable compared with that found using the AAV antisense strategy, without the potential disadvantages of toxic or immunological effects attributable to the vector. Mechanistic insight and further structure-activity studies are likely to identify improved peptides for transvascular cardiac AO transduction. Whether restoration of cardiac dystrophin protein to 20% of normal levels is likely to be adequate to regain or maintain normal cardiac function is unknown and further studies will be required, particularly in DMD animal models manifesting a significant cardiac phenotype, e.g. dystrophin and utrophin deficient DKO mice (36) or the golden retriever dog model. However in DMD patients, the degree to which cardiac function is regained or maintained will depend not only on the level of dystrophin protein restored but also on the particular BMD-like dystrophin isoform restored by exon skipping in each case, given that the BMD cardiac phenotype is highly heterogeneous (14,37).

Our data showed widespread, uniform, high-level dystrophin protein expression in all *mdx* peripheral muscle groups studied, including central abdominal wall and diaphragm muscles, 3 weeks following treatment with a single 25 mg/kg PMO-peptide dose. Many muscle groups demonstrated dystrophin protein restored to levels in excess of 50% of normal, significantly higher than that reported previously using naked PMO compounds (4) or estimated in the first

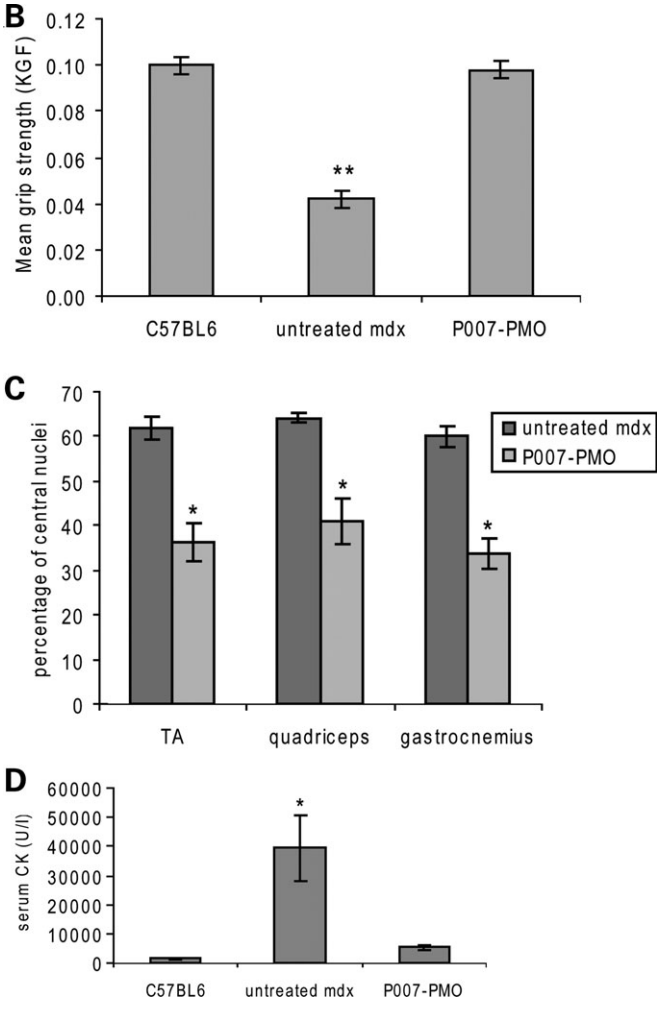

Figure 3. Continued

human clinical study with direct intramuscular delivery of 2′*O*-methyl phosphorothioate AOs (11). As a consequence we found that DAPC protein components were efficiently re-localized, muscle histology appeared normal and muscle grip strength was restored to within the normal range. RT-PCR analysis using a nested reaction at 25 cycles revealed that for all tissues except the heart, virtually all mutant transcripts had been successfully skipped suggesting the possibility of AO-target saturation. We therefore tested whether or not a lower dose of PMO-peptide conjugate could effectively restore dystrophin expression. While near normal levels of dystrophin protein were restored in peripheral muscles with this lower dose, central muscles including diaphragm and heart were less well corrected at dystrophin and DAPC protein levels. The question therefore arises as to the optimal dosing regime of PMO-peptide AOs. Given our data at the high 25 mg/kg dose, that the estimated half-life of dystrophin protein approaches 26 weeks in *mdx* mice (18,19) and that peptide conjugates are known to increase PMO tissue uptake and retention (38,39), a single higher PMO-peptide threshold dose followed by lower maintenance doses at 4–8 week intervals may be optimal. Further studies will be required to determine this and to evaluate the longer-term functional and physiological effects of this treatment.

MATERIALS AND METHODS

Animals

Six-to-eight-week old *mdx* mice were used in all experiments (six mice in the test and four in control groups). The experiments were carried out in the Animal unit, Department of Physiology, Anatomy and Genetics, University of Oxford, Oxford, UK according to procedures authorized by the UK Home Office. Mice were killed by CO_2 inhalation or cervical dislocation at desired time points, and muscles and other tissues were snap-frozen in liquid nitrogen-cooled isopentane and stored at −80°C.

PMO and PMO-peptide conjugates

Details of PMO and PMO-peptide conjugates are shown in Table 1. Conjugations of peptide with PMO were synthesized by a stable amide linker as described elsewhere (40). All conjugates are synthesized by AVI Biopharma Inc. (Corvallis, OR, USA). The PMO AO sequence against the boundary sequences of exon and intron 23 of the dystrophin gene was 5′-ggccaaacctcggcttacctgaaat-3′, and designated as 25mer PMO (M23D).

RNA extraction and nested RT-PCR analysis

Total RNA was extracted from skeletal muscle and heart tissue with Trizol (Invitrogen, UK) and 200 ng of RNA template was used for 20 μl RT-PCR with OneStep RT-PCR kit (Qiagen, UK). The primer sequences for the initial RT-PCR were Exon20Fo 5′-CAGAATTCTGCCAATTGCTGAG-3′ and Ex26Ro 5′-TTCTTCAGCTTGTGTCATCC-3′ for amplification of messenger RNA from exons 20 to 26. The cycle conditions were 95°C for 30 s, 55°C for 1 min and 72°C for 2 min for 25 cycles. RT-PCR product (1 μl) was then used as the template for secondary PCR performed in 25 μl with 0.5U *Taq* DNA polymerase (Invitrogen, UK). The primer sequences for the second round were Ex20Fi CCCAGTCTACCACCCTATCAG AGC-3′ and Ex24Ri 5′-CAGCCATCCATTTCTGTAAGG -3. The cycle conditions were 95°C for 1 min, 57°C for 1 min and 72°C for 2 min for 25 cycles. The products were examined by electrophoresis on a 2% agarose gel.

Intramuscular and systemic injection of PMO-peptide conjugates

For intramuscular studies the TA muscle of each experimental *mdx* mouse was injected with a 40 μl dose of PMO–peptide conjugates with saline at a final concentration of 125 μg/ml, and the contralateral muscle was injected with saline. For systemic intravenous injections, 500 μg PMO-peptide conjugates in 80 μl saline buffer were injected into tail vein of mdx mice at the final dose of 25 mg/kg and 6 mg/kg, respectively. The animals were killed at various time points after injection by CO_2 inhalation and tissues were removed and snap-frozen in liquid nitrogen-cooled isopentane and stored at −80°C.

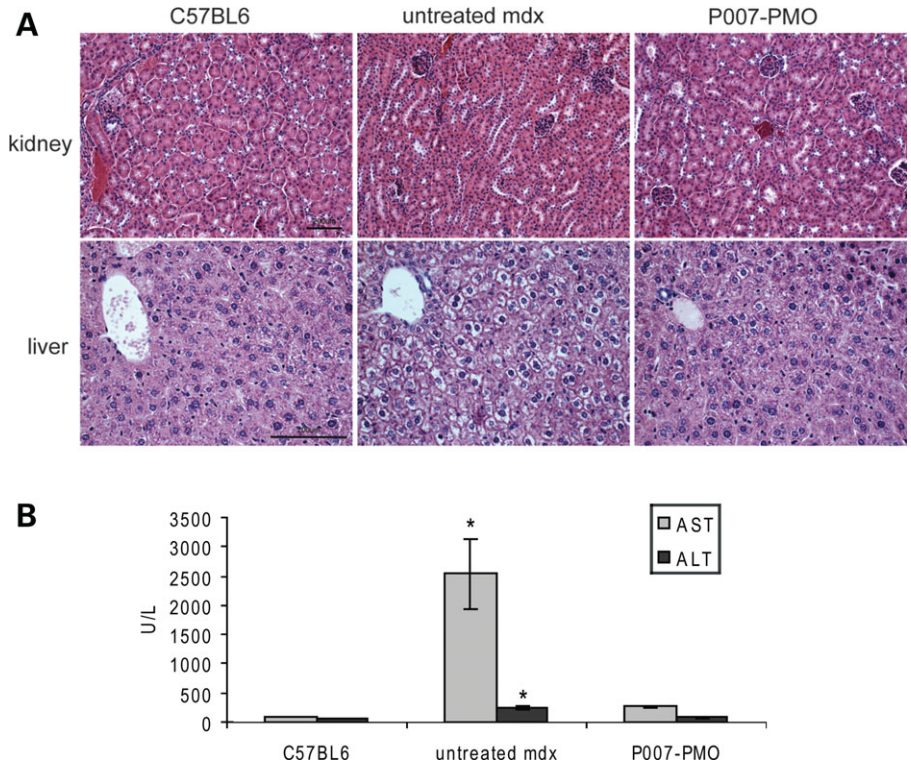

Figure 4. Histological and clinical biochemistry measures of systemic toxicity in *mdx* mice treated with the P007-PMO conjugate. (**A**) Haematoxylin and eosin staining of kidney (upper panel) and liver (lower panel) tissues sections from treated *mdx* mice, untreated *mdx* mice and C57BL6 normal controls (scale bar = 200 μm). Tissue sections from renal cortex show normal glomerular and tubule tissue architecture in P007-PMO treated and control mice. Liver sections show normal hepatic tissue morphology in control C57BL6 mice, evidence of mild microvacuolar cellular change (indicated by arrows) in untreated *mdx* hepatocytes and partial reversal of this cellular change in P007-PMO treated mdx mice, which show near normal liver histology. (**B**) Measurement of serum levels of aspartate aminotransferase (AST) and alanine aminotransferase (ALT) liver enzymes in treated *mdx* mice compared with normal and untreated *mdx* mice. Data shows improved pathological parameters in P007-PMO treated *mdx* mice compared with untreated controls with significantly lower serum levels of both enzymes ($n = 6$ for treated group and $n = 4$ for control, $P < 0.05$).

Immunohistochemistry and histology

Sections of 8 μm were cut from at least two-thirds of the muscle length of TA, quadriceps, gastrocnemius, biceps, abdominal wall and diaphragm muscles and cardiac muscle at 100 μm intervals. The sections were then examined for dystrophin expression with a polyclonal antibody 2166 against the dystrophin C-terminal region (the antibody was kindly provided by Professor Kay Davies). The maximum number of dystrophin-positive fibres in one section was counted using the Zeiss AxioVision fluorescence microscope. The intervening muscle sections were collected either for RT-PCR analysis and western blot or as serial sections for immunohistochemistry. Polyclonal antibodies were detected by goat-anti-rabbit IgGs Alexa Fluro 594 (Molecular Probe, UK). Routine haematoxylin and eosin staining was used to examine overall muscle morphology and assess the level of infiltrating mononuclear cells. The serial sections were also stained with a panel of polyclonal and monoclonal antibodies for the detection of DAPC protein components. Rabbit polyclonal antibody to neuronal nitric oxide synthase (nNOS) and mouse monoclonal antibodies to β dystroglycan, α-sarcoglycan and β-sarcoglycan were used according to manufacturer's instructions (Novocastra, UK). Polyclonal antibodies were detected by goat-anti-rabbit IgGs Alexa 594 and the monoclonal antibodies by goat-anti-mouse IgGs Alexa 594 (Molecular Probe, UK). The M.O.M. blocking kit (Vector laboratories, Inc. Burlingame, CA) was applied for the immunostaining of the DAPC.

Centrally nucleated fibre counts

TA, quadriceps and gastrocnemius muscles from *mdx* mice treated with PMO-peptide conjugates were examined. To ascertain the number of centrally nucleated muscle fibres, sections were stained for dystrophin with rabbit polyclonal antibody 2166 and counter-stained with DAPI for cell nuclei (Sigma, UK). About 500 dystrophin positive fibres for each tissue sample were counted and assessed for the presence of central nuclei using a Zeiss AxioVision fluorescence microscope. Fibres were judged centrally nucleated if one or more nuclei were not located at the periphery of the fibre. Untreated age-matched *mdx* mice were used as controls.

Protein extraction and western blot

The collected sections were placed in a 1.5 ml polypropylene eppendorf tube (Anachem, UK) on dry ice. The tissue sections were lysed with 150 μl protein extraction buffer containing 125 mmol/l Tris–HCl (pH = 6.8), 10% sodium dodecyl

sulphate, 2 mol/l urea, 20% glycerol and 5% 2-mercaptoethanol. The mixture was boiled for 5 min and centrifuged. The supernatant was collected and the protein concentration was quantified by Bradford assay (Sigma, UK). Various amounts of protein from normal C57BL6 mice as a positive control and corresponding amounts of protein from muscles of treated or untreated *mdx* mice were loaded onto sodium dodecyl sulphate polyacrylamide gel electrophoresis gels (4% stacking, 6% resolving). Samples were electrophoresed for 4 h at 80 mA and transferred to nitrocellulose overnight at 50 V at 4°C. The membrane was then washed and blocked with 5% skimmed milk and probed overnight with DYS1 (monoclonal antibody against dystrophin R8 repeat, 1:200, NovoCastra, UK) for the detection of dytstrophin protein and α-actinin (monoclonal antibody, 1:5000, Sigma, UK) as a loading control. The bound primary antibody was detected by horseradish peroxidise-conjugated rabbit anti-mouse IgGs and the ECL Western Blotting Analysis system (Amersham Pharmacia Biosciences, UK). The intensity of the bands obtained from treated *mdx* muscles was measured by Image J software; the quantification is based on band intensity and area, and is compared with that from normal muscles of C57BL6 mice.

Functional grip strength analysis

Treated mice and control mice were tested using a commercial grip strength monitor (Chatillon, UK). Each mouse was held 2 cm from the base of the tail, allowed to grip a protruding metal triangle bar attached to the apparatus with their forepaws, and pulled gently until they released their grip. The force exerted was recorded and five sequential tests were carried out for each mouse, averaged at 30 s apart.

Serum creatinine kinase measurements and other biochemical tests

Serum and plasma were taken from the mouse jugular vein immediately after the killing with CO_2 inhalation. Analysis of serum CK, AST, ALT, urea and creatinine levels was performed by the clinical pathology laboratory (Mary Lyon Centre, Medical Research Council, Harwell, Oxfordshire, UK).

Statistical analysis

All data are reported as mean values $\pm$SEM. Statistical differences between treatment groups and control groups were evaluated by SigmaStat (Systat Software, UK) and one-tailed *t*-test was applied.

SUPPLEMENTARY MATERIAL

Supplementary Material is available at *HMG* Online.

FUNDING

This work was supported by UK Department of Health and the UK Muscular Dystrophy Campaign.

ACKNOWLEDGEMENTS

The authors would like to thank the UK MDEX Consortium for helpful discussions and support. They would also like to thank Professor Kay Davies, Department of Physiology, Anatomy and Genetics, University of Oxford for providing access to facilities including the *mdx* mouse colony; Dr Tertius Hough, Clinical Pathology Laboratory, Mary Lyon Centre, MRC, Harwell, UK for clinical testing of blood samples; and Christine Simpson, Department of Physiology, Anatomy and Genetics, University of Oxford for assistance with histology.

Conflict of Interest statement. None declared.

REFERENCES

1. Hoffman, E.P., Brown, R.H. Jr. and Kunkel, L.M. (1987) Dystrophin: the protein product of the Duchenne muscular dystrophy locus. *Cell*, **51**, 919–928.
2. England, S.B., Nicholson, L.V., Johnson, M.A., Forrest, S.M., Love, D.R., Zubrzycka-Gaarn, E.E., Bulman, D.E., Harris, J.B. and Davies, K.E. (1990) Very mild muscular dystrophy associated with the deletion of 46% of dystrophin. *Nature*, **343**, 180–182.
3. Aartsma-Rus, A., Kaman, W.E., Weij, R., den Dunnen, J.T., van Ommen, G.J. and van Deutekom, J.C. (2006) Exploring the frontiers of therapeutic exon skipping for Duchenne muscular dystrophy by double targeting within one or multiple exons. *Mol. Ther.*, **14**, 401–407.
4. Alter, J., Lou, F., Rabinowitz, A., Yin, H., Rosenfeld, J., Wilton, S.D., Partridge, T.A. and Lu, Q.L. (2006) Systemic delivery of morpholino oligonucleotide restores dystrophin expression bodywide and improves dystrophic pathology. *Nat. Med.*, **12**, 175–177.
5. Gebski, B.L., Mann, C.J., Fletcher, S. and Wilton, S.D. (2003) Morpholino antisense oligonucleotide induced dystrophin exon 23 skipping in mdx mouse muscle. *Hum. Mol. Genet.*, **12**, 1801–1811.
6. Aartsma-Rus, A., Janson, A.A., Kaman, W.E., Bremmer-Bout, M., den Dunnen, J.T., Baas, F., van Ommen, G.J. and van Deutekom, J.C. (2003) Therapeutic antisense-induced exon skipping in cultured muscle cells from six different DMD patients. *Hum. Mol. Genet.*, **12**, 907–914.
7. Aartsma-Rus, A., Janson, A.A., Kaman, W.E., Bremmer-Bout, M., van Ommen, G.J., den Dunnen, J.T. and van Deutekom, J.C. (2004) Antisense-induced multiexon skipping for Duchenne muscular dystrophy makes more sense. *Am. J. Hum. Genet.*, **74**, 83–92.
8. Lu, Q.L., Mann, C.J., Lou, F., Bou-Gharios, G., Morris, G.E., Xue, S.A., Fletcher, S., Partridge, T.A. and Wilton, S.D. (2003) Functional amounts of dystrophin produced by skipping the mutated exon in the mdx dystrophic mouse. *Nat. Med.*, **9**, 1009–1014.
9. Lu, Q.L., Rabinowitz, A., Chen, Y.C., Yokota, T., Yin, H., Alter, J., Jadoon, A., Bou-Gharios, G. and Partridge, T. (2005) Systemic delivery of antisense oligoribonucleotide restores dystrophin expression in body-wide skeletal muscles. *Proc. Natl Acad. Sci. USA*, **102**, 198–203.
10. Mann, C.J., Honeyman, K., Cheng, A.J., Ly, T., Lloyd, F., Fletcher, S., Morgan, J.E., Partridge, T.A. and Wilton, S.D. (2001) Antisense-induced exon skipping and synthesis of dystrophin in the mdx mouse. *Proc. Natl Acad. Sci. USA*, **98**, 42–47.
11. van Deutekom, J.C., Janson, A.A., Ginjaar, I.B., Frankhuizen, W.S., Aartsma-Rus, A., Bremmer-Bout, M., den Dunnen, J.T., Koop, K., van der Kooi, A.J., Goemans, N.M. *et al.* (2007) Local dystrophin restoration with antisense oligonucleotide PRO051. *N. Engl. J. Med.*, **357**, 2677–2686.
12. Wilton, S.D., Fall, A.M., Harding, P.L., McClorey, G., Coleman, C. and Fletcher, S. (2007) Antisense oligonucleotide-induced exon skipping across the human dystrophin gene transcript. *Mol. Ther.*, **15**, 1288–1296.
13. Yin, H., Lu, Q. and Wood, M. (2008) Effective exon skipping and restoration of dystrophin expression by peptide nucleic acid antisense oligonucleotides in mdx mice. *Mol. Ther.*, **16**, 38–45.
14. McNally, E.M. (2007) New approaches in the therapy of cardiomyopathy in muscular dystrophy. *Annu. Rev. Med.*, **58**, 75–88.
15. Finsterer, J. and Stollberger, C. (2003) The heart in human dystrophinopathies. *Cardiology*, **99**, 1–19.

16. Abes, R., Arzumanov, A., Moulton, H., Abes, S., Ivanova, G., Gait, M.J., Iversen, P. and Lebleu, B. (2008) Arginine-rich cell penetrating peptides: Design, structure-activity, and applications to alter pre-mRNA splicing by steric-block oligonucleotides. *J. Pept. Sci.*, **14**, 455–460.
17. Moulton, H.M., Fletcher, S., Neuman, B.W., McClorey, G., Stein, D.A., Abes, S., Wilton, S.D., Buchmeier, M.J., Lebleu, B. and Iversen, P.L. (2007) Cell-penetrating peptide-morpholino conjugates alter pre-mRNA splicing of DMD (Duchenne muscular dystrophy) and inhibit murine coronavirus replication *in vivo*. *Biochem. Soc. Trans.*, **35**, 826–828.
18. Fletcher, S., Honeyman, K., Fall, A.M., Harding, P.L., Johnsen, R.D., Steinhaus, J.P., Moulton, H.M., Iversen, P.L. and Wilton, S.D. (2007) Morpholino oligomer-mediated exon skipping averts the onset of dystrophic pathology in the mdx mouse. *Mol. Ther.*, **15**, 1587–1592.
19. Ahmad, A., Brinson, M., Hodges, B.L., Chamberlain, J.S. and Amalfitano, A. (2000) Mdx mice inducibly expressing dystrophin provide insights into the potential of gene therapy for duchenne muscular dystrophy. *Hum. Mol. Genet.*, **9**, 2507–2515.
20. Blake, D.J., Weir, A., Newey, S.E. and Davies, K.E. (2002) Function and genetics of dystrophin and dystrophin-related proteins in muscle. *Physiol. Rev.*, **82**, 291–329.
21. Tinsley, J.M., Blake, D.J., Zuellig, R.A. and Davies, K.E. (1994) Increasing complexity of the dystrophin-associated protein complex. *Proc. Natl Acad. Sci. USA*, **91**, 8307–8313.
22. Brenman, J.E., Chao, D.S., Gee, S.H., McGee, A.W., Craven, S.E., Santillano, D.R., Wu, Z., Huang, F., Xia, H., Peters, M.F. *et al.* (1996) Interaction of nitric oxide synthase with the postsynaptic density protein PSD-95 and alpha1-syntrophin mediated by PDZ domains. *Cell*, **84**, 757–767.
23. Newey, S.E., Benson, M.A., Ponting, C.P., Davies, K.E. and Blake, D.J. (2000) Alternative splicing of dystrobrevin regulates the stoichiometry of syntrophin binding to the dystrophin protein complex. *Curr. Biol.*, **10**, 1295–1298.
24. Fowler, S.C., Zarcone, T.J., Chen, R., Taylor, M.D. and Wright, D.E. (2002) Low grip strength, impaired tongue force and hyperactivity induced by overexpression of neurotrophin-3 in mouse skeletal muscle. *Int. J. Dev. Neurosci.*, **20**, 303–308.
25. Oliver, P.L., Keays, D.A. and Davies, K.E. (2007) Behavioural characterisation of the robotic mouse mutant. *Behav. Brain Res.*, **181**, 239–247.
26. Qiao, C., Li, J., Jiang, J., Zhu, X., Wang, B., Li, J. and Xiao, X. (2008) Myostatin propeptide gene delivery by adeno-associated virus serotype 8 vectors enhances muscle growth and ameliorates dystrophic phenotypes in mdx mice. *Hum. Gene Ther.*, **19**, 241–254.
27. Fabb, S.A., Wells, D.J., Serpente, P. and Dickson, G. (2002) Adeno-associated virus vector gene transfer and sarcolemmal expression of a 144 kDa micro-dystrophin effectively restores the dystrophin-associated protein complex and inhibits myofibre degeneration in nude/mdx mice. *Hum. Mol. Genet.*, **11**, 733–741.
28. Wells, D.J., Wells, K.E., Walsh, F.S., Davies, K.E., Goldspink, G., Love, D.R., Chan-Thomas, P., Dunckley, M.G., Piper, T. and Dickson, G. (1992) Human dystrophin expression corrects the myopathic phenotype in transgenic mdx mice. *Hum. Mol. Genet.*, **1**, 35–40.
29. Glesby, M.J., Rosenmann, E., Nylen, E.G. and Wrogemann, K. (1988) Serum CK, calcium, magnesium, and oxidative phosphorylation in mdx mouse muscular dystrophy. *Muscle Nerve*, **11**, 852–856.
30. Brazeau, G.A., Mathew, M. and Entrikin, R.K. (1992) Serum and organ indices of the mdx dystrophic mouse. *Res. Commun. Chem. Pathol. Pharmacol.*, **77**, 179–189.
31. Jearawiriyapaisarn, N., Moulton, H.M., Buckley, B., Roberts, J., Sazani, P., Fucharoen, S., Iversen, P.L. and Kole, R. (2008) Sustained dystrophin expression induced by peptide-conjugated morpholino oligomers in the muscles of mdx mice. *Mol. Ther*, **16**, 1624–1629.
32. Townsend, D., Yasuda, S., Li, S., Chamberlain, J.S. and Metzger, J.M. (2008) Emergent dilated cardiomyopathy caused by targeted repair of dystrophic skeletal muscle. *Mol. Ther.*, **16**, 832–835.
33. Gregorevic, P., Allen, J.M., Minami, E., Blankinship, M.J., Haraguchi, M., Meuse, L., Finn, E., Adams, M.E., Froehner, S.C., Murry, C.E. *et al.* (2006) rAAV6-microdystrophin preserves muscle function and extends lifespan in severely dystrophic mice. *Nat. Med.*, **12**, 787–789.
34. Blankinship, M.J., Gregorevic, P. and Chamberlain, J.S. (2006) Gene therapy strategies for Duchenne muscular dystrophy utilizing recombinant adeno-associated virus vectors. *Mol. Ther.*, **13**, 241–249.
35. Goyenvalle, A., Vulin, A., Fougerousse, F., Leturcq, F., Kaplan, J.C., Garcia, L. and Danos, O. (2004) Rescue of dystrophic muscle through U7 snRNA-mediated exon skipping. *Science*, **306**, 1796–1799.
36. Tinsley, J.M., Potter, A.C., Phelps, S.R., Fisher, R., Trickett, J.I. and Davies, K.E. (1996) Amelioration of the dystrophic phenotype of mdx mice using a truncated utrophin transgene. *Nature*, **384**, 349–353.
37. Duan, D. (2006) Challenges and opportunities in dystrophin-deficient cardiomyopathy gene therapy. *Hum. Mol. Genet.*, **15** (Spec no. 2), R253–R261.
38. Lebleu, B., Moulton, H.M., Abes, R., Ivanova, G.D., Abes, S., Stein, D.A., Iversen, P.L., Arzumanov, A.A. and Gait, M.J. (2008) Cell penetrating peptide conjugates of steric block oligonucleotides. *Adv. Drug Deliv. Rev.*, **60**, 517–529.
39. Burrer, R., Neuman, B.W., Ting, J.P., Stein, D.A., Moulton, H.M., Iversen, P.L., Kuhn, P. and Buchmeier, M.J. (2007) Antiviral effects of antisense morpholino oligomers in murine coronavirus infection models. *J. Virol.*, **81**, 5637–5648.
40. Wu, R.P., Youngblood, D.S., Hassinger, J.N., Lovejoy, C.E., Nelson, M.H., Iversen, P.L. and Moulton, H.M. (2007) Cell-penetrating peptides as transporters for morpholino oligomers: effects of amino acid composition on intracellular delivery and cytotoxicity. *Nucleic Acids Res.*, **35**, 5182–5191.